THREE-DIMENSIONAL ANALYSIS OF CHARGING EVENTS ON DAYS 87 and 114, 1979, FROM SCATHA

N. A. Saflekos
Boston College

M. F. Tautz
Radex Corporation

A. G. Rubin and D. A. Hardy
Air Force Geophysics Laboratory

P. F. Mizera
The Aerospace Corporation

J. Feynman
Boston College

SUMMARY

Detailed observations of angular distributions of ions and electrons from the SCATHA (Spacecraft Charging at High Altitudes) SC-5 experiment were used to investigate the floating potential and the differential charging of the spacecraft as deduced from Liouville's theorem and computed by the NASCAP/AFGL code. The highest resolution data from the SCATHA SSPM experiment were compared to the SC-5 charged particle fluxes and to the NASCAP/AFGL computations. This study led to the following conclusions: a) Short-time charging events on the spacecraft are associated with short-time increases of the intensity of 10 keV to 1 MeV electrons, b) Short time changes of the spacecraft differential potential are associated with simultaneous short-time changes of the spacecraft floating potential, c) Solar U.V. intensities in penumbra, as monitored by the solar panels total current, anticorrelate with the spacecraft floating potentials, d) Based on the measured profiles of U.V intensities, NASCAP predicts correct forms of sun-shade asymmetric surface potentials consistent with the SSPM measurements, e) Certain enhancements of the intensity of energetic ions (E_i>100 keV) have been observed to diminish the absolute value of the spacecraft surface potential, f) Spacecraft discharging events in times shorter than 20 sec have been observed without obvious changes in the spectrum of the energetic (E > 10 keV) plasma, g) Partial discharging of the spacecraft has occasionally been observed upon entry into a magnetically depleted region, h) Steady state potentials and transient potentials of duration less than 30 seconds have been successfully simulated by the NASCAP code.

INTRODUCTION

Operational spacecraft (S/C) experience a host of anomalies which vary from nuisance to fatality. It is believed that electrostatic charging events are responsible for some of these anomalies especially at high altitudes and at the popular commercial belt, the geosynchronous orbit. At low altitudes in the absence of intense field-aligned currents (FAC) a high concentration of cold ionospheric plasma keeps the S/C floating potential at a small negative value. The situation however, changes for the worse when FAC's with increased densities strike the surface area of a large structure. Large structures then charge up to kilovolt potential levels which may constitute a serious hazard to such S/C orbiting the earth at lower polar altitudes.

Observed fast discharges can generate large amplitude current pulses on power or S/C ground lines and destroy sensitive solid state devices. To avoid such costly losses, it is highly desirable to enhance our understanding of surface material properties and to develop servomechanisms which will actively control the S/C potential. Perhaps the emission of energetic ion beams together with neutralizing cold electrons is a satisfactory control system. NASA and the USAF, using their experience from the SCATHA (S/C Charging at High Altitudes) satellite, hope to study the charging characteristics important to the design of solar power satellites and other space-based large structures.

The SCATHA spacecraft is an integral part of a mission that interests physicists and engineers alike whose goal is the prevention of spacecraft charging. SCATHA, otherwise designated as satellite P78-2, was launched into a near-geosynchronous orbit on 30 January 1979. By 2 February 1979, the orbit was adjusted to conform to a period of 23.597 hours, a perigee of 27,517 km and apogee of 43,192 km and an inclination of 7.09°. The P78-2 satellite spins at the rate of about 1 rpm with the spin axis pointing along the direction of the vector S X Z where S points towards the sun and Z along the geographic north axis.

Figure 1 shows the P78-2 S/C payload. Of particular interest to this work are two experiments which measure the S/C potentials with one second resolution. They are designated as SC-1 and SC-5. Both of these instruments are described in full detail in (ref. 1). The SC-1 experiment, otherwise known as SSPM (Spacecraft Surface Potential Monitor), consists of three separate instruments (SSPM-1,-2 and-3) which provide measurements of the surface voltage and the bulk current of S/C insulating and conducting materials frequently used in S/C construction. Redundant measurements of aluminized kapton are made on each of the three instruments (SC1-1, SC1-2, and SC1-3) see Figure 2. The SC1-3 sample is mounted on the top plane of the S/C having its normal parallel to the S/C spin axis. The other two samples, mounted near the equator of the rotating S/C, spend about thirty seconds in darkness and thirty seconds in light during one spin period while not in the earth's shadow. The front surface potential of the samples is derived from the back surface potential using laboratory calibration curves.

The SC-5 instrument scans rapidly through the spectrum of electrons from 50 eV to 1.1 MeV and of protons from 50 eV to 35 MeV. The rapid scan particle detectors measure the differential charged particle flux parallel and perpendicular to the S/C spin axis. From the full pitch angle information in one plane, one derives temperatures, number densities, and bulk flow velocities. From energy dependent pitch angle anisotropies in the distribution, one can infer the occurrence of S/C charging.

In a cooperative effort NASA and the U.S. Air Force have supported the effort of S^3 (Systems, Science and Software, Inc.) which developed a charging analyzer program known by a combination of acronyms as NASCAP/AFGL. This code simulates the electrostatic charging of a three dimensional object at geosynchronous environments. More specifically, an object is introduced into the program by defining the geometrical and electrical properties of the structural materials with considerable complexity. Then the object is allowed to interact with a magnetospheric plasma in darkness or in light. Having at its disposal the object definition and the description of the ambient plasma, the program solves a fully three dimensional problem involving Poisson's equation. The charge distribution on the spacecraft surfaces is calculated from the total current to the spacecraft taking into account proton and electron incidence, backscattering, and secondary emission (electrons only). NASCAP/AFGL has excellent graphics for object representation, external potential contours, and external space charge density contours.

The code obtains these results by following an alternating procedure where in every step it calculates the charge accumulation and the resulting electrostatic potential on each S/C surface. The calculations can be made in the presence of ambient magnetic and electric fields. As an option, the code can do a first order photosheath analysis. More details can be found in (ref. 2) and references therein. In this paper we present some detailed observations and model calculations which lead to the conclusions that the results from SSPM, SC5, and the NASCAP code are internally and logically consistent.

CHARGING IN ECLIPSE

On day 87, 1979 SCATHA entered the earth's penumbra at 1615:26 UT (Universal Time) and the earth's umbra at 1618:38 UT. The spacecraft did not show a change of its charging state until 1635:00 UT. In the previous half hour the energetic electrons ($10 \leq E_e < 58$ keV) were two to three orders of magnitude lower in counting rate in comparison with the averge in the preceding two hours. At 16:36 UT the auroral AE index rose suddenly, reaching a value of 1000 nT (1nT = 10^{-5} gauss). To within forty seconds of this time, the energetic electron counting rate rose above the preceding dropout levels by about one order of magnitude. For the following five minutes, the charged particle fluxes, the S/C ground potential, and the S/C differential potential all underwent fast (seconds) temporal variations.

Figure 3 shows data from the SC5 and the SC1 experiments on SCATHA.

The top panel shows sun angle and pitch angle for the SC5 electron detector parallel to the S/C spin axis. The middle panel shows the electron fluxes for eight channels identified by their energies and a shift number N in decades needed to separate the traces. The lower panel left scale refers to the SSPM voltage of the samples on top of the satellite. The scale on the right refers to the magnitude of the total real field as measured by the magnetometer SC-11 on SCATHA. The electron measurements were taken at a fixed (90°) pitch angle. At about 1636:12 UT we noted a continuous increase in the flux of energy $E_e \leq 8.97$ keV while the fluxes of energy $E_e > 8.97$ keV dropped more abruptly. The more energetic particles reached their peak at 1637 UT whereas the less energetic ones reached their minimum value at about 1638 UT. This flux dependence on energy can be understood in terms of S/C charging where the buildup of negative charge on the S/C inhibits the current flow away from the S/C. It took under two minutes for the S/C ground to reach a negative voltage between -4.57 and -8.97 kV. The average value is -6.8 kV. At 1638 UT, SC9 reported a value of -8.14 kV and SC2 reported the value of -6.9 kV. Our value agrees very well with SC2 and is consistent with the value of SC9.

Later in the plot the lower energy particles recovered during two short UT intervals (1638:40 - 1639:10 and 1639:40 - 1640:00). The 0.1 keV electrons recovered in the first time interval but not in the second. Thus we would place the first S/C ground potential at 0.1 kV and the second at 0.3 kV. The SC9 experiment reported a 0.45 kV and 1.2 kV S/C ground potentials for the two intervals above.

In bottom panel of Figure 3, the 3V3 trace corresponds to the front surface voltage of the quartz fabric sample. A change of its charging state commenced at 1636:40 UT corresponding to the peaking of $E_e = 23.2$ keV electrons. The 3V2 trace corresponds to silvered teflon sample. It responded five seconds later coinciding with the peaking of $E_e = 52.7$ keV electron fluxes. Both samples continued to charge linearly in time up until 1638:40 UT. Then both samples partially discharged for thirty seconds keeping in phase with the S/C ground discharging in the same time interval. A similar event was repeated in the interval between 1639:40 and 1640:00 UT. It is interesting to note that the magnetic field strength was significantly reduced during the first S/C discharge. Perhaps the magnetometer sensed a current surge on the S/C surface of the kind that would cause damage to solid state devices. The magnetometer saw a lesser current flow in the second interval (1639:40 - 1640:00) UT.

Figure 4 is similar to Figure 3 except for more energetic electrons. The increase of the fluxes at the onset of differential charging is obvious. The responding SSPM sample 1V1 is aluminized kapton. It began charging at 1636:30, about ten seconds earlier than the commencement of charging in Figure 3, which corresponds to peaking of electron flux in the energy range $E_e < 23.2$ keV. Kapton also partially discharged during the 1638:40 to 1639:10 UT interval. The minimum differential charging of kapton was about -1750 volts at 1640:20 UT. At that same time interval, silvered teflon of Figure 3 reached about -1500 volts. The other two SSPM samples are: optical solar reflector (1V3) and gold (1V4). Both remained less negative than -200

volts. There is a striking difference in the behavior of the surface potentials between materials placed on top and materials placed near the equator of the spacecraft. The differences cannot be resolved by energy dependent pitch angle anisotropies. Other phenomena causing time dependent behavior of the electrical properties of the materials must be studied more intensively.

In addition to the more accurate representation of the SCATHA object (Figure 2, four grid model) in the NASCAP/AFGL code, the program accepts simpler models roughly approximating the realistic three-dimensional representation of the satellite. In order to study effects of space plasma on the S/C in the absence of sunlight, we selected a test object in the shape of a quasisphere, a figure with 26 sides inscribed in a sphere as shown in Figure 5. All the surfaces are covered with goldpd, a grounded conductor, except for four squares facing the +Y direction covered with silicon dioxide, teflon, gold, and kapton, all allowed to float relative to S/C ground. The four patches are meant to represent the SC1 sample materials. The gold sample is decoupled from the underlying conductor via a large capacitor.

Figure 6 shows the steady state potentials assumed by the S/C ground (goldpd) and the four samples mentioned above using space plasma temperatures and densities derived from the SC5 experiment. We selected those spectra during eclipse when the S/C ground voltage was at a low negative level. We fit the selected spectra with two Maxwellian distributions in the ranges 0.1 to 2 keV and 2 to 60 keV. The resulting temperatures and densities were averaged in the separate energy intervals. The low energy range temperatures and densities for electrons and protons respectively were (Te_1 = 0.338 keV, n_{e1} = 0.12 cm^{-3}) and (T_{p1} = 0.207 keV, n_{p1} = 0.62 cm^{-3}). Similarly the higher energy range parameters were (T_{e2} = 9.74 keV, n_{e2} = 0.38 cm^{-3}) and (T_{p2} = 6.09 keV, n_{p2} = 0.47 cm^{-3}). The kapton sample thickness was set at 1.27×10^{-3}m and its bulk conductivity at $\sigma = 1 \times 10^{-14}$ mho/m. The decoupling capacitor for gold was set at $C_{ij} = 5 \times 10^{-9}$F and the grid mesh X_{mesh} was set at 0.5m to make the model total volume comparable to that of the real spacecraft. Figure 6 shows that goldpd (S/C ground) charged to -1689 volts. The average S/C ground voltage from 1634:54 to 1715:54 UT was -2771 volts as derived from SC9 ion counting rate data provided by Eldon Whipple of UCSD. In a later time interval from 1703:53 to 1715:54, the average S/C ground potential was -2063 volts differing only by a 17% from the NASCAP/AFGL code calculated value for goldpd. The differential charging for the four samples relative to goldpd were (-2505, -1453, -20, and +65) volts for (kapton, teflon, silicon dioxide (SIO2), and gold), respectively. The largest negative values measured by the SSPM experiment were (-1700, -2150, -1100, and -200) volts for (1V1 (kapton), 3V2 (teflon), 3V3 (SIO2), and IV4 (gold)), respectively. Except for SIO2 which the code predicts, like goldpd, the potentials less than -200 volts are predicted to within a factor of two of the experimental values.

SPACECRAFT CHARGING DURING ENTRY INTO ECLIPSE

On Day 114, 1979 SCATHA entered the earth's penumbra at 0710:10 UT and was eclipsed totally at 0713:26 UT. During the penumbral transit the solar illumination diminished by atmospheric scattering of sunlight and the S/C photocurrent was decreased in direct proportion. A temporal variation of the S/C photocurrent resulted in a variation of the S/C ground potential. Figure 7 shows the directional differential intensity of ions with energy E_p= 9.66 keV, the directional differential intensity of electrons with energy E_e = 4.42 keV and their respective pitch angle all plotted versus UT. The intensity of the 90° fluxes and the nature of the dependence of flux on pitch angle change drastically around 0713 UT. The electron flux following this time is generally reduced by a factor of 2 whereas the proton flux is generally increased by factors of 4. The electron flux anisotropy becomes deeper after 0713 UT maintaining a ratio of perpendicular to parallel fluxes of about 2 for at least seven minutes. In contrast the proton fluxes anti-correlate with the electron fluxes and they maintain a ratio of parallel to perpendicular number fluxes of about 5. The simultaneity of solar UV decrease with this acceleration of ions and deceleration of electrons argues in favor of a S/C charging event whereby the potential reached about -7 kV capable of affecting the E_p = 9.66 keV and the E_e = 4.42 keV channels. The fact that the ions (electrons) are preferentially accelerated (decelerated) along the 0° and the 180° pitch angles (D • B; where, D and B are unit vectors with D being the detector look direction and B being the direction of the magnetic field) argues against a single localized potential drop parallel to the magnetic field at a latitude other than that of the S/C on the same field lines.

Figure 8 shows distributions from the SC5 rapid scanning particle detectors (RSPD's) parallel to the S/C spin axis during the precharging period at about 0706 UT and during the charging period at about 0717 UT. One readily observes that the electron distribution functions are shifted to lower energies by about 4 keV and the ions to higher energies by about 8 keV. Due to the wide energy windows of the channels $\Delta E/E \simeq 1$, we cannot specify the S/C potential very accurately using this method. The SC-9 experiment with better energy resolution reported a S/C ground potential of about -5 kV at around 0717 UT. This result is consistent with our inferred S/C ground potential relative to plasma ground. Single Maxwellian fits of the distributions in Figure 8 overestimate the temperatures of lower energy plasma ($5 < E < 25$ keV). For that reason we chose a plasma about two times colder than that at 0706 UT and assumed it does not change throughout the penumbral transit. The temperatures and densities for electrons and protons, respectively, were (T_e = 6.4 keV, n_e = 0.8 cm^{-3}) and (T_p = 5.8 keV, n_p = 0.5 cm^{-3}). This information was then fed into the NASCAP/AFGL code for the quasisphere model. The program was allowed to run until it reached equilibrium surface potentials. Then we turned the solar intensity on as a function of time but now with the time reversed. Figure 9 shows the eight minute calculations of S/C ground (goldpd) potential, insulator (teflon) potential, and insulator (kapton) potential going backwards in time from 0714 UT to 0706 UT. One clearly observes that the transient nature of the potentials resembles the transmitted curve of sunlight through the atmosphere plotted against the

impact parameter. The S/C ground and the insulating materials surface voltages respond to solar UV as soon as the solar illumination level reaches 20%. The spin modulation of the surface potentials of teflon and kapton samples are due to S/C shadowing. During eclipse, teflon and kapton reached -1900 and -4900 volts lower than goldpd. In full sunlight, this computer run showed that teflon discharged almost completely reaching -50 volts in comparison to the +5 volts of goldpd. Kapton maintained a minimum of -800 volts in S/C shadow and a maximum of -80 volts in full sunlight. We did not have measurements of S/C differential charging to compare with these results.

SPACECRAFT CHARGING DURING EXIT FROM ECLIPSE

On Day 87, 1979 SCATHA was coming out of total eclipse at 1713:50 UT and left the penumbra at 1716:10 UT. Figure 10, lower panel, shows the solar illumination and four SCATHA SSPM voltages as a function of time. The middle panel shows plots of electron fluxes from the SC5 instrument with field of view perpendicular to the S/C spin axis. The top panel shows the angles between the detector line of sight and the magnetic field and between the detector line of sight and the satellite-sun-line. The relative variation of the solar illumination was measured by the total current of the solar panels. This illumination was also compared to theoretical predictions and was found to be in excellent agreement. Figure 10, middle panel, shows the isotropic electrons $E_e < 9.16$ keV to increase with the solar illumination following the time 1714:30 UT at which point the solar illumination has approached its 20% value. The rate of recovery of the electrons $E_e = 4.42$ keV is slow in comparison to the lower energy channels. Thus the S/C potential at the onset of photodischarge was around three thousand volts which is roughly obtained by averaging the 4.42 and 1.57 keV energy channels. We reiterate the wide energy windows of the electron channels $\Delta E/E \simeq 1$ do not allow an accurate estimate of the S/C ground potential relative to plasma ground. The angular resolution of the SC5 experiment, on the other hand, is excellent and Figure 10 upper two panels show that after 1715:50 UT the electron directional differential fluxes for all the presented channels were isotropic in the satellite spin plane. Thus it is believed that all the SSPM samples experienced the same incident electron flux. The SSPM-2 (Figure 10, lower panel) responded to sunlight immediately following 1714:20 UT. The minimum potentials relative to S/C ground that the SSPM's had prior to entering penumbra were (-500, -1650, -200, and -300) volts for (kapton with hole, kapton large sample, reference band, and reference band with high gain) respectively.

In order to simulate the transient behavior of the S/C surface potentials as SCATHA came out of total eclipse, we used the NASCAP/AFGL code with the quasisphere model described in the preceding section. We calculated a two Maxwellian environment from distribution functions in the time interval 1716:00 to 1716:47 UT. The energy spectra were chosen in a fixed pitch angle interval $80° < \alpha < 90°$. The spectra were also restricted to ones

corresponding to S/C ground potentials greater than -100 volts so that shifting in energy would not have been a factor. Thus we averaged sixteen electron and ion distribution functions separately and computed temperatures and densities of

$(T_{e1} = 731$ eV, $n_{e1} = 0.78$ cm^{-3}, $T_{e2} = 6.4$ keV, $n_{e2} = 0.79$ cm$^{-3})$

for electrons and $(T_{p1} = 198$ eV, $n_{p1} = 0.8$ cm^{-3}, $T_{p2} = 5.8$ keV,

$n_{p2} = 0.5$ cm$^{-3})$ for protons.

The Maxwellian fits were made in the energy ranges $100 < E < 4570$ eV and $4570 < E < 60000$ eV. The higher energy population was not subtracted from the lower energy population samples. The actual environment used in the NASCAP/AFGL computer run was similarly derived from an average of 55 spectra which yielded

$(T_{e1} = 338$ eV, $n_{e1} = 0.12$ cm^{-3}, $T_{e2} = 9.74$ keV, $n_{e2} = 0.38$ cm$^{-3})$

for electrons and $(T_{p1} = 207$ eV, $n_{p1} = 0.62$ cm^{-3}, $T_{p2} = 6.09$ keV,

$n_{p2} = 0.47$ cm$^{-3})$ for protons.

Figure 11 shows the temporal variation of the surface potential of the large kapton sample (SC1-2-2) (Ref. 2) together with the surface voltages of teflon and S/C ground (goldpd). The trace light intensity represents the relative solar illumination of SCATHA obtained from the solar panels total current as described in a previous section. The prepenumbral value of the kapton voltage relative to S/C ground was -2527 volts. Clearly as the sun intensity increases, the kapton voltage grows less negative and shows a modulation once per spin period. This again is due to S/C shadowing of the kapton sample. The conductivity and thickness of this material were 10^{-14} mho/m and 10 times the nominal thickness, respectively. Comparing the SSPM value of -1650 volts to the NASCAP/ AFGL value of -2527 volts, we see that they differ by 35%. The agreement can become better if good knowledge of the S/C ground potential (down to a few volts) is used to correct the distribution functions. Furthermore, measurement of the environment with higher energy resolution may give the temperature and densities more accurately. When very high energy points (hundreds of keV) are included in the distribution functions, the temperatures are overestimated. Figure 12 is included in this study in order to show the effect of high energy protons on S/C charging.

Figure 12, top panel shows pitch angles and sun angles of the SC5 perpendicular protons whose fluxes and energies are given in the figure. The middle panel is similar to the top except for parallel protons. The bottom panel shows the SSPM-1 surface voltages together with the solar illumination versus time. Prior to 1714:10 UT the SSPM sample potentials were flat. At that time a sudden enhancement of the energetic proton flux (up by a factor of 30) appears to have initiated the gradual discharge of the SSPM1-1 (kapton) and the SSPM1-4 (gold). This flux increase did not affect the charging rates of the SSPM1-2 (optical solar reflector, OSR, grounded to

the S/C chassis) and the SSPM1-3, an ungrounded OSR. At 1714:30 UT, twenty seconds later, the parallel protons of the same energy showed a similar flux increase. The delayed arrival of proton enhancements did not affect the charging rates of the SSPM1 on the bellyband. Perhaps it affected the SSPM1-3 on the top of the S/C but that set of data has not been studied yet. The proton flux profiles shown in Figure 12 indicate that the particles peaked in ten seconds and arrived from two different azimuthal directions. The first increase arrived from a direction perpendicular to the satellite-sun vector and the satellite velocity. The second increase arrived from the ram direction. The asymmetry is explainable by a north-south boundary of energetic protons moving eastward. If we assume that the boundary was 1 gyroradius thick (220 km for 126 keV protons), then this boundary was moving with a velocity of 11 km/sec eastward and slightly away from the earth. Such motions may take place during the decay phase of subtorms. Ground magnetograms show that the AL index was rapidly decreasing at the time of arrival of the energetic protons. In contrast to the proton weak discharging effect, the SSPM-1 sample responded rapidly to the fast photo-discharging at 1714:40 UT when the solar illumination reached its 20% level.

SPACECRAFT CHARGING IN FULL SUNLIGHT

Normally the S/C ground remains at potential levels close to zero or slightly positive when the sun shines on the S/C. This is achieved by the solar UV produced photocurrent. However, occasionally the ambient plasma becomes hard enough to cause charging of shaded insulators to potential levels lower than those of S/C ground. Figure 13 is similar to Figure 10 only in sunlight. The top and middle panels show that the electrons from .11 keV to 53.8 keV are isotropic. Starting with 1316:30 UT, the electrons with energies $4.42 < E_e < 53.8$ keV increase whereas the electrons with energies $0.11 < E_e < 4.42$ keV decrease. This is an indication that the S/C entered the plasma sheet region in a period of about 20 seconds. In this case, the absence of low energy electrons does not imply S/C charging. Figure 13, bottom panel, shows that the SSPM1-1 (kapton) responded to differential charging and it reached its extreme value at around 1317:45 UT. A similar S/C charging phenomenon is observed on samples looking in the ram direction. Figure 14, middle panel, shows the energetic electrons from the SC5 parallel to the spin axis detector and bottom panel shows the SSPM-3 samples with normals parallel to the S/C velocity vector. The electron signature of a local acceleration event is similar to that of Figure 13. The SSPM-3-2 (teflon) begins to respond differentially at 1316:50 UT as does the SSPM-3-3 (quartz fabric). The sample of gold (SSPM-3-4) did not show a change in its charge state. The SSPM-3 is not spin modulated as it is constantly in S/C shadow during this orbit. Finally, we would like to include a figure of NASCAP/AFGL calculations which shows quite satisfactorily that the highest spatial resolution model of SCATHA in the code produces results of differential charging in excellent agreement with experimental results.

On Day 114, 1979 (April 24, 1979) from about 0650:40 UT to about 200 seconds later SCATHA was rotating in full sunlight (see Figure 15). Using SC5 data during the pre-eclipse period on this day (see Figure 7), we assumed no charging and fitted the particle phase space densities to single Maxwellians. This fit resulted in temperatures and densities of (T_e = 10 keV, n_e = 1 cm^{-3} for electrons) and (T_p = 10 keV, n_p = 0.5 cm^{-3} for protons). Figure 15 upper panel shows the surface voltage of the SSPM-2-2 samples (large kapton), with thickness 10 times the nominal thickness as calculated by the NASCAP/AFGL code, during three rotations of SCATHA in sunlight. The lower panel shows the spin modulated surface potential of the SSPM-2-2 measurements. The charging rates are in excellent agreement. The discharging rates in each cycle do not match exactly as indicated by the different slopes in the upper and lower panels. This means that the electrical and mechanical properties of the kapton sample need fine tuning. Such an effort should be made after studying S/C charging under many different environments. The theoretical and the experimental results, nevertheless, agree in aplitude and phase in a striking way. We take this agreement to mean that the modeling of SCATHA by the NASCAP/AFGL computer code is valid.

CONCLUDING REMARKS

We have presented experimental and theoretical results on S/C charging in full sunlight, during eclipse entry, during total eclipse, and during exit from eclipse. Our principal findings are summarized in the abstract. In order to make further progress in validating the NASCAP/AFGL code, more data are needed from several experiments simultaneously including the ion and electron gun emissions. In addition, the model is in need of better defined materials properties for the monitored samples and for the rest of the materials distributed on the SCATHA surfaces shown in Figure 2.

REFERENCES

1. Description of the Space Test Program P78-2 Spacecraft and Payloads. Editors: John R. Stevens and Alfred L. Vampola, 1978.

2. A Three-Dimensional Spacecraft - Charging Computer Code, Allen G. Rubin, Ira Katz, Myron Mandell, Gary Schnuelle, Paul Steen, Don Parks, Jack Cassidy, and James Roche, in Space Systems and Their Interactions with Earth's Space Environment, edited by Henry B. Garrett and Charles P. Pike, Vol. 71 of Progress in Astronautics and Aeronautics.

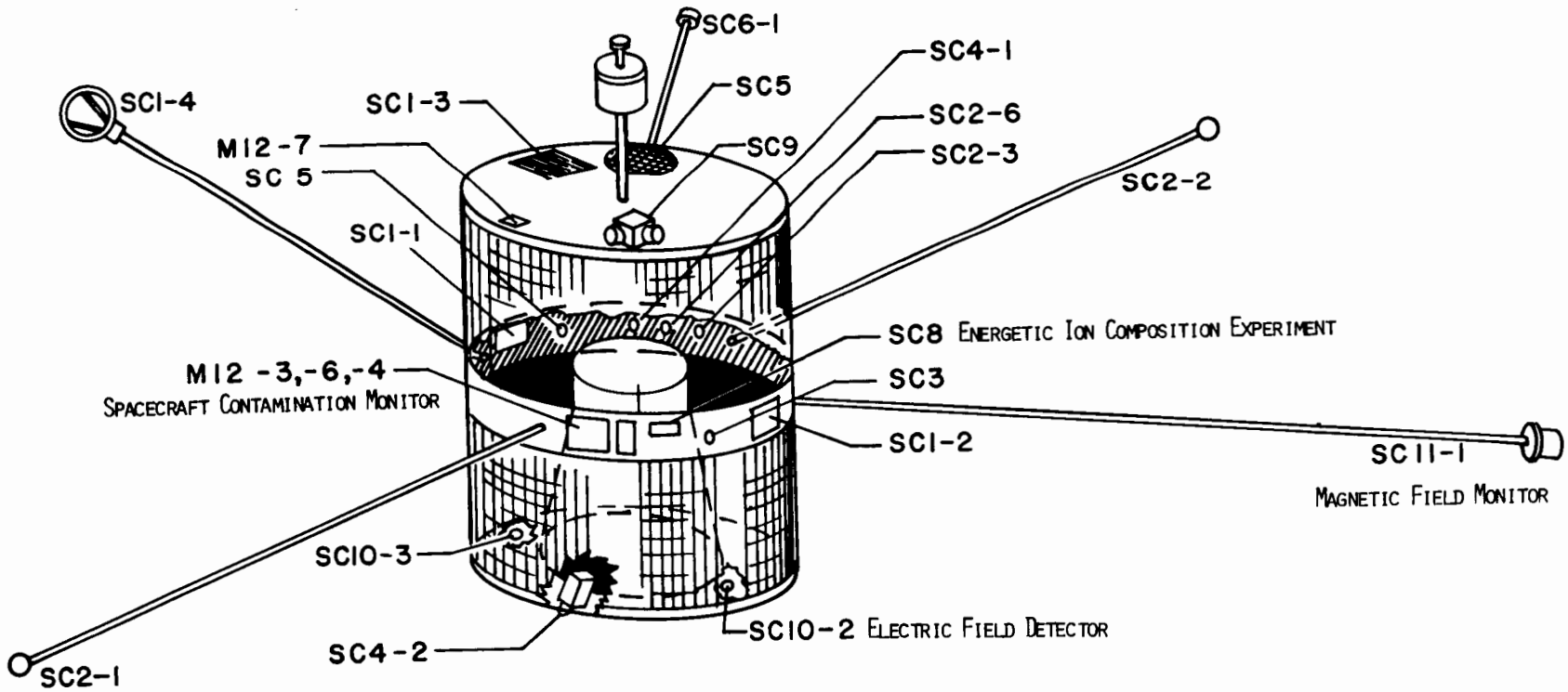

SC1 Radio Frequency Electromagnetic Wave Anlyzer
SC1 Very Low Frequency Electromagnetic Wave Analyzer
SC1 Satellite Surface Potential Monitor
SC1 Pulse Shape Analyzer
SC2 Energetic Proton Detectors
SC2 Spacecraft Sheath Potential Monitor

SC3 High Energy Particle Spectrometer
SC4-1 Electron Beam System
SC4-2 Positive Ion Beam System
SC5 Rapid Scan Particle Detector
SC6 Thermal Plasma Analyzer
SC7 Light Ion Mass Spectrometer
SC9 UCSD Charged Particle Experiment

Figure 1. SCATHA spacecraft payload.

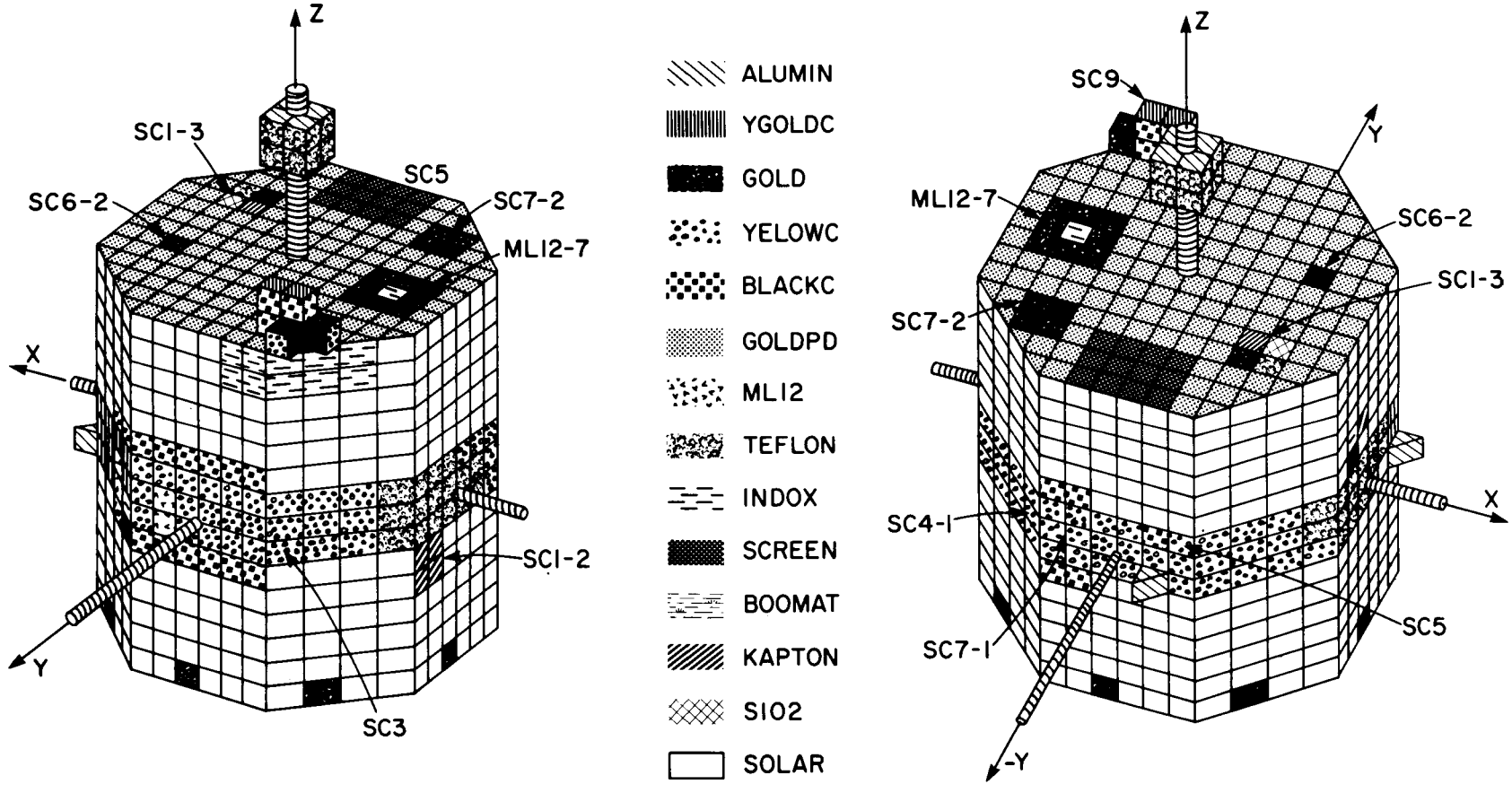

Figure 2. Materials distribution on the surface of the SCATHA satellite. NASCAP graphics generated figures shaded by hand.

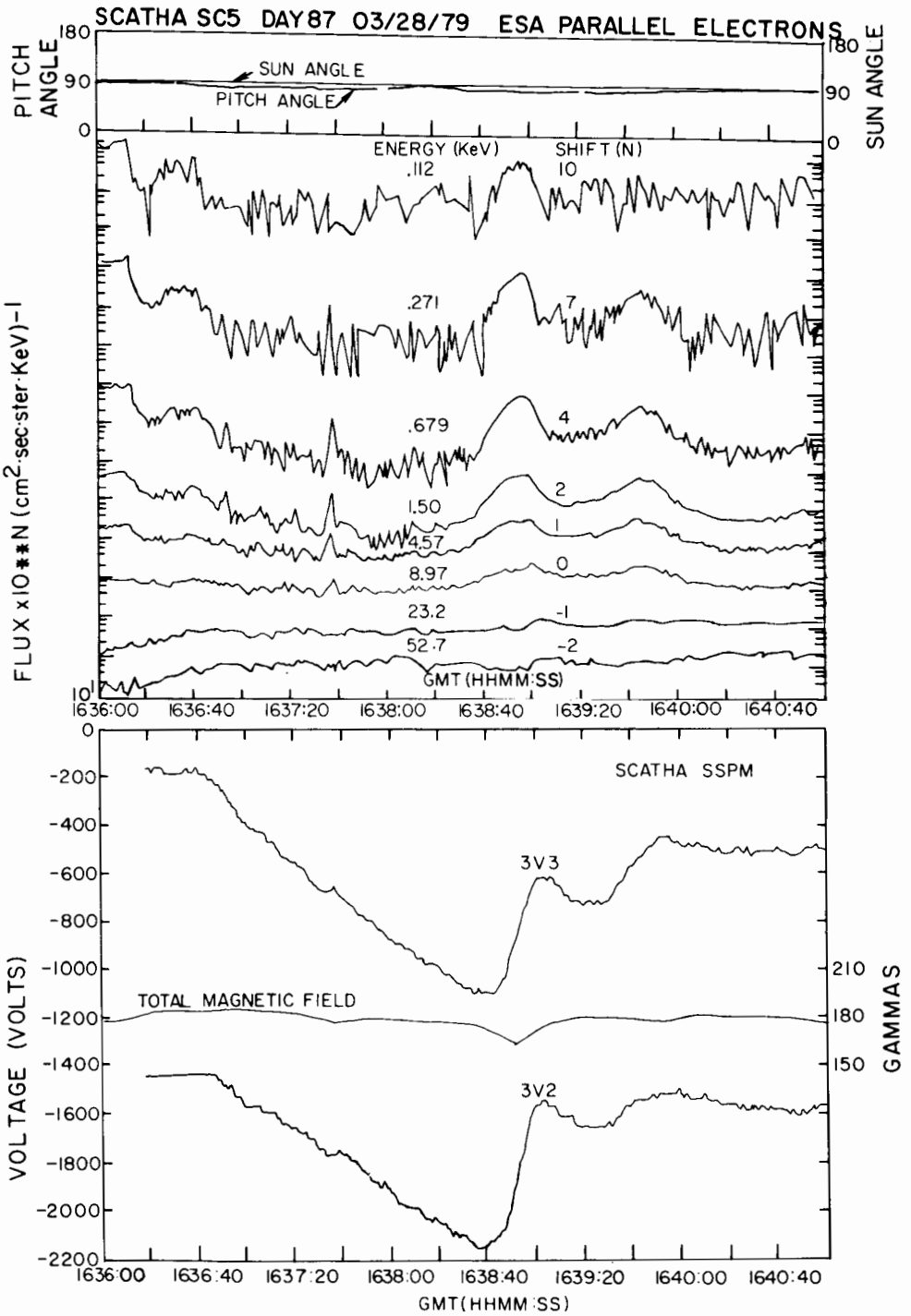

Figure 3. Spacecraft attitude, parallel electron fluxes, surface potentials, and ambient magnetic field plotted versus Greenwich Mean Time (UT).

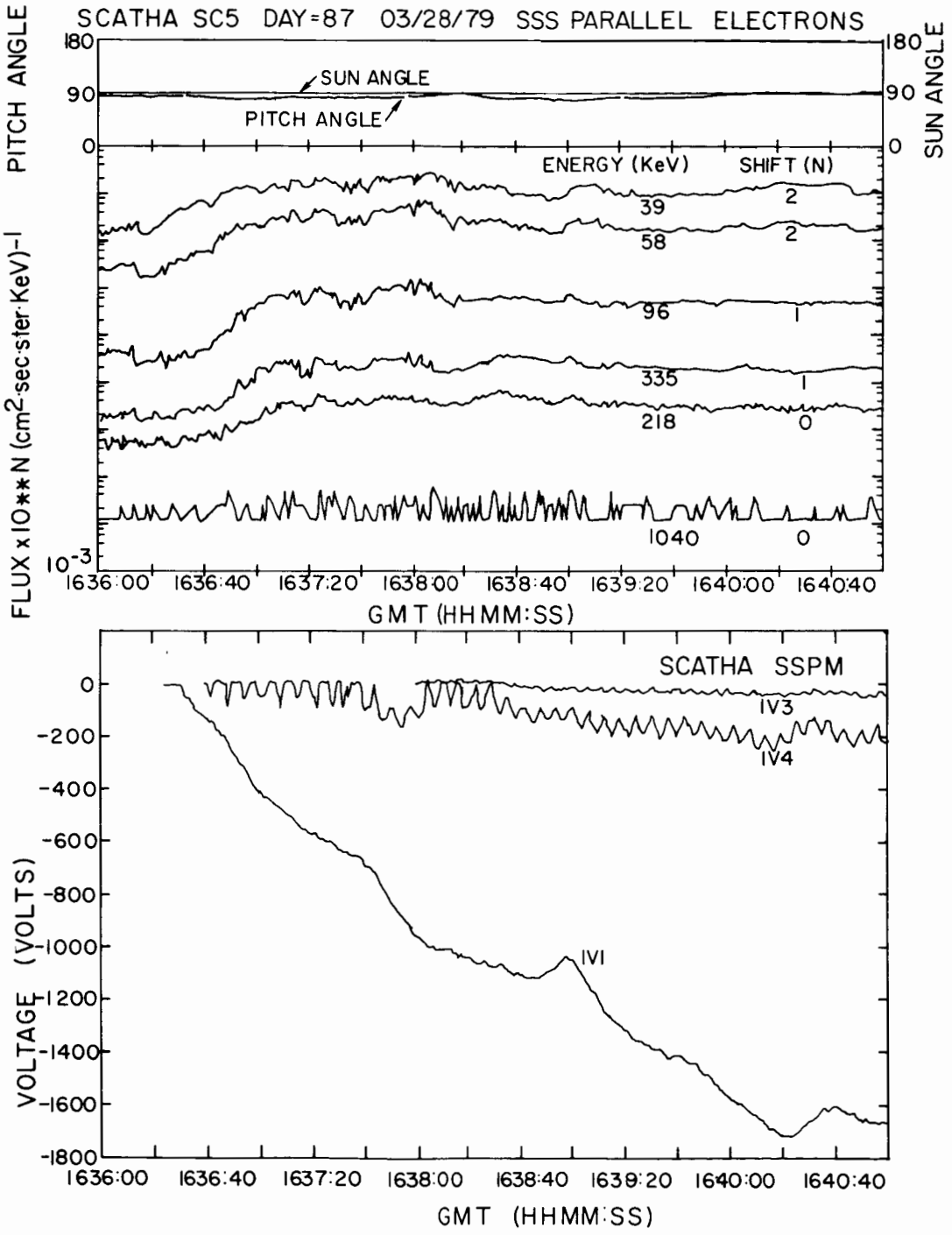

Figure 4. Same as Figure 3 only for more energetic electrons, different surface sample and without magnetic field.

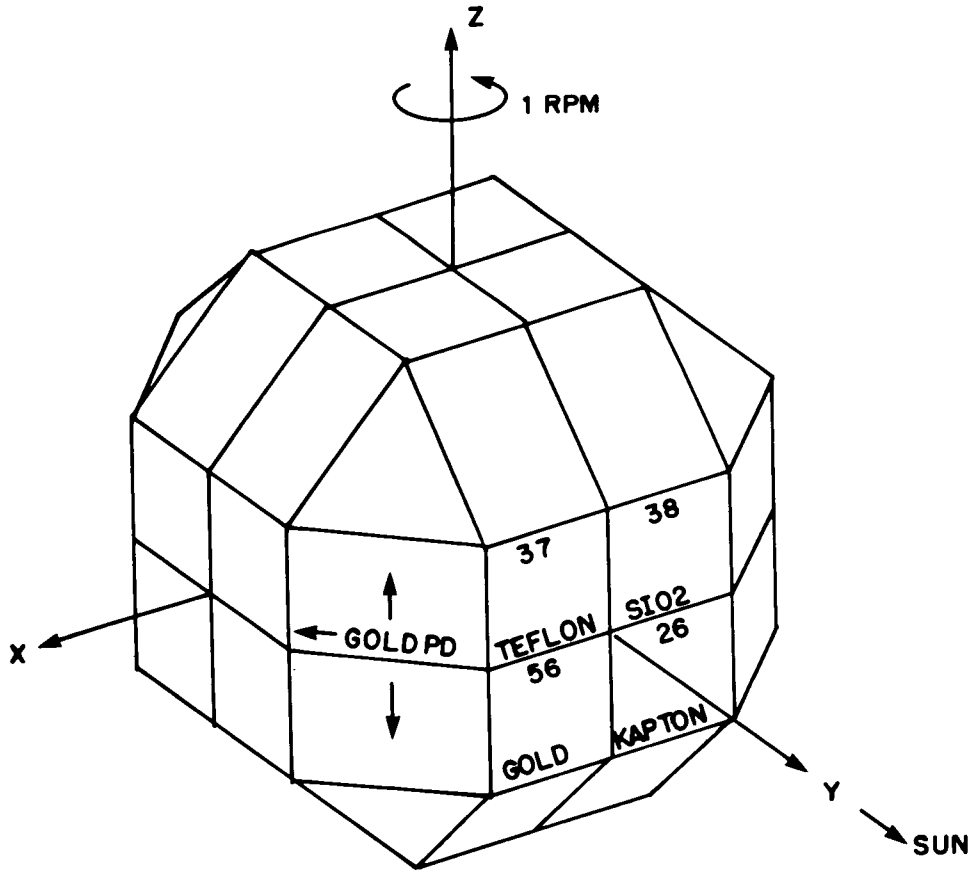

Figure 5. A quasispherical object modeled by the NASCAP/AFGL code.

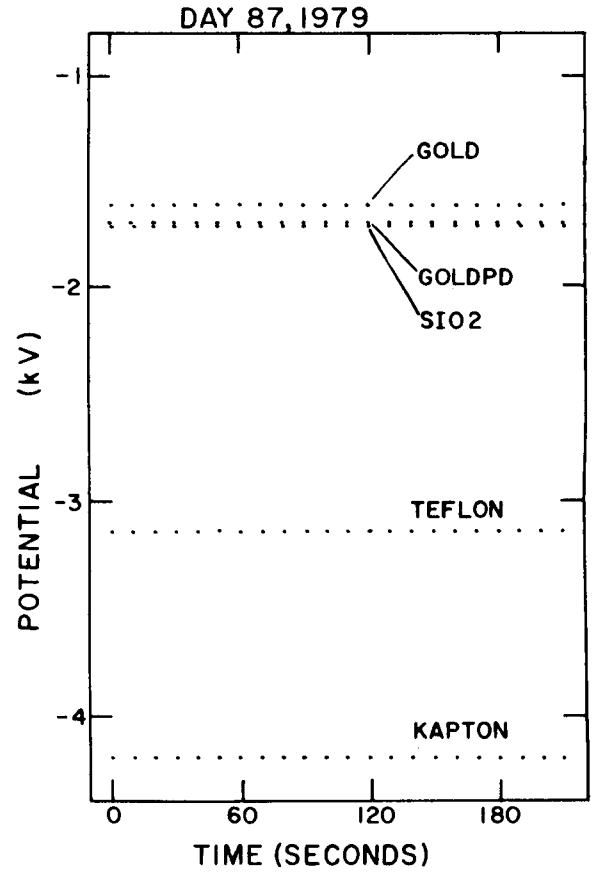

Figure 6. Spacecraft surface potentials simulated by the NASCAP/AFGL computer code.

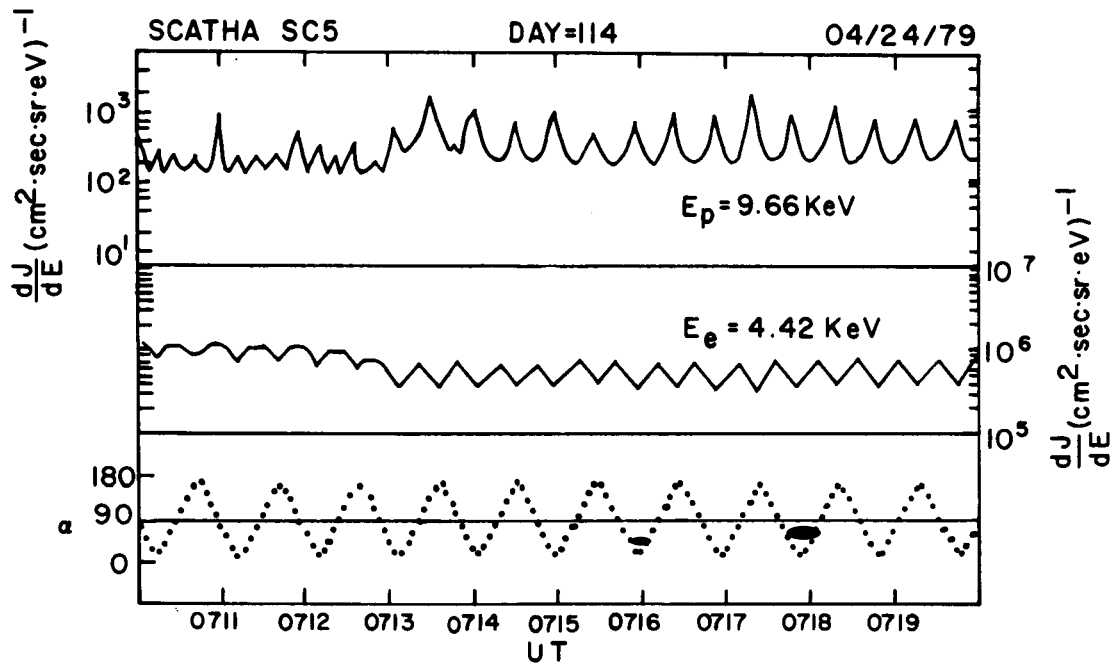

Figure 7. Directional differential intensities for ions (E_p = 9.66 keV) and electrons (E_e = 4.42 keV) together with their pitch angles all plotted versus universal time.

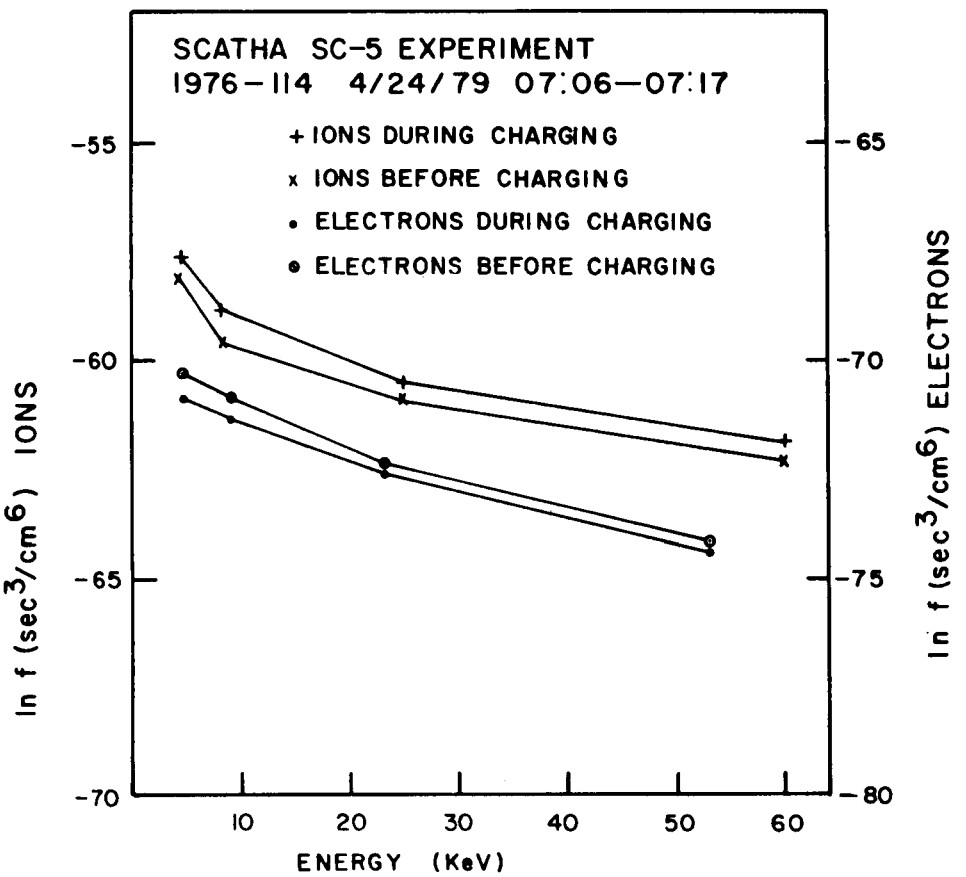

Figure 8. Ion and electron distribution functions versus energy at 0706 and 0717 UT on day 114, 1979 from the SCATHA SC5 experiment.

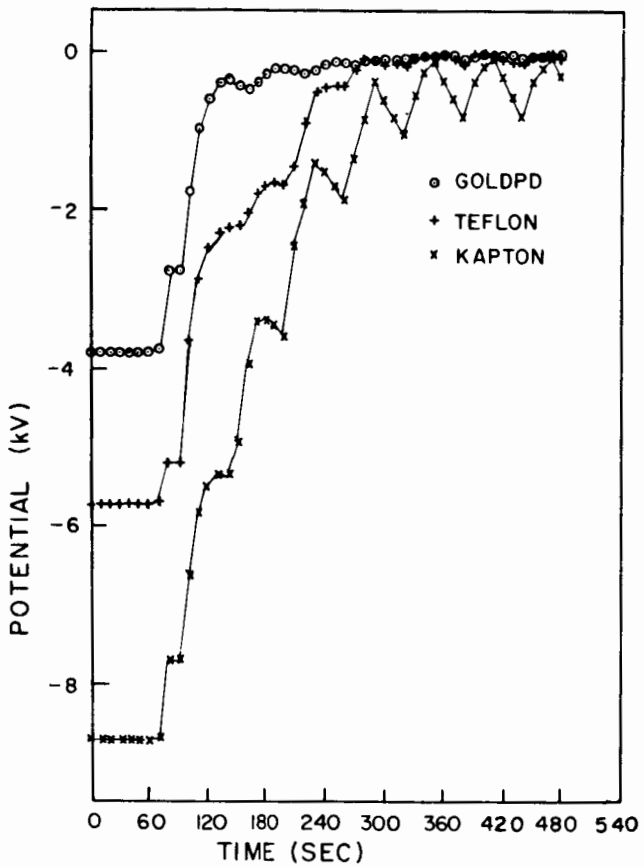

Figure 9. Spacecraft surface potentials simulated by the NASCAP/AFGL computer code.

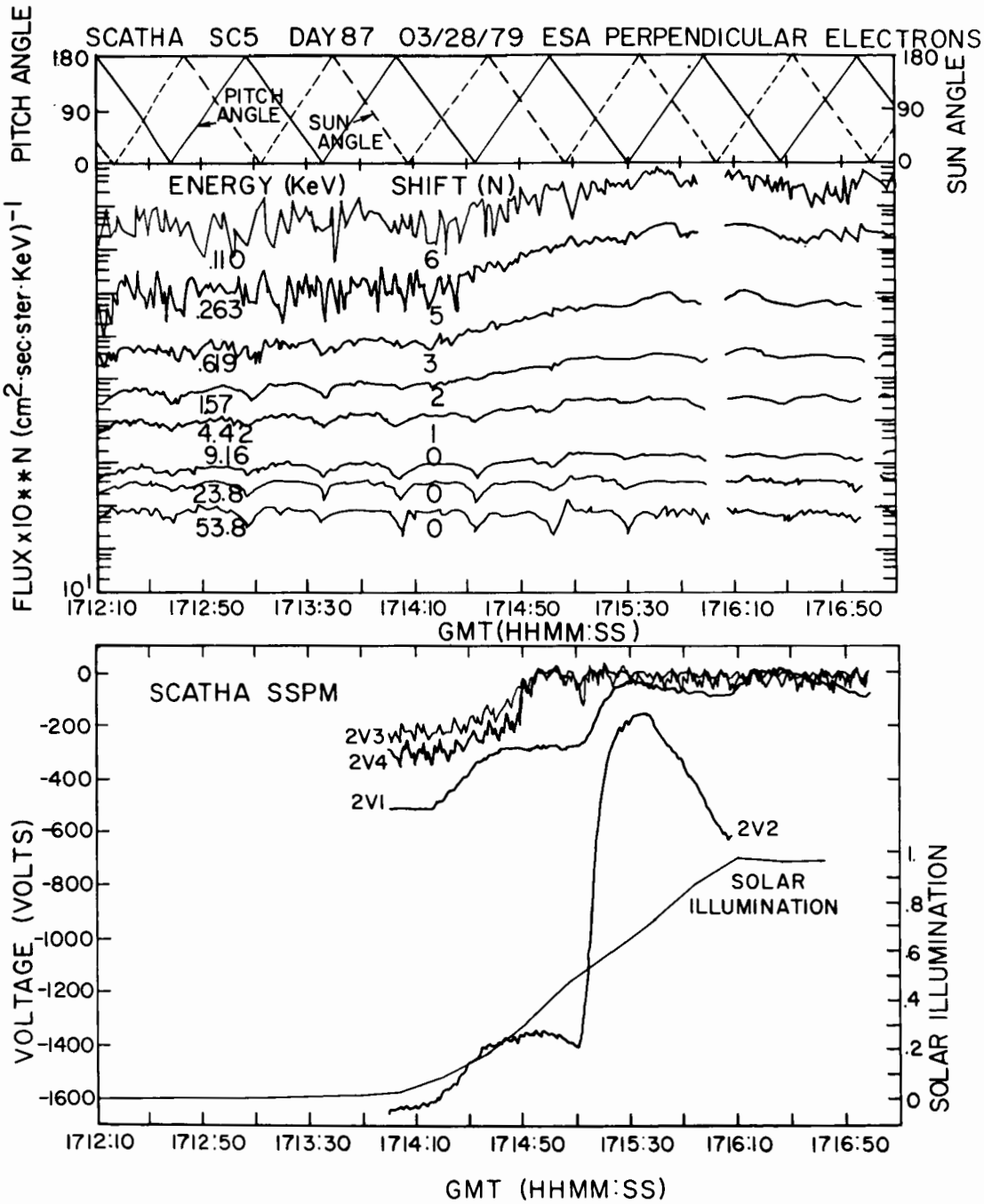

Figure 10. Top panel, pitch angle and sun-angle of SC5 perpendicular detector. Middle panel, directional differential intensities for eight channels each shifted by N decades to resolve the traces. Bottom panel, SCATHA SSPM-2 voltages and solar illumination. All traces plotted versus universal time GMT.

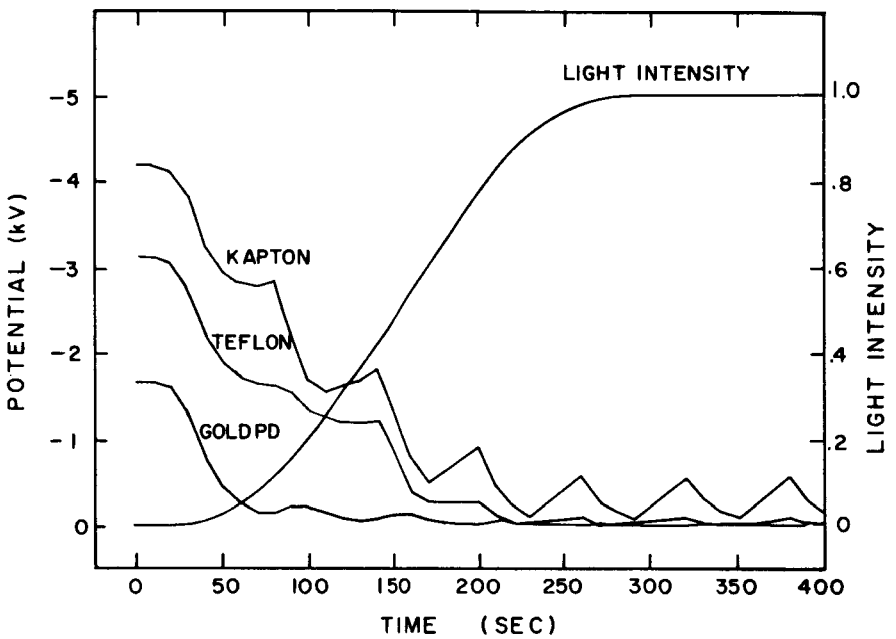

Figure 11. Similar to Figure 9 except for day 87, 1979 during exit from eclipse.

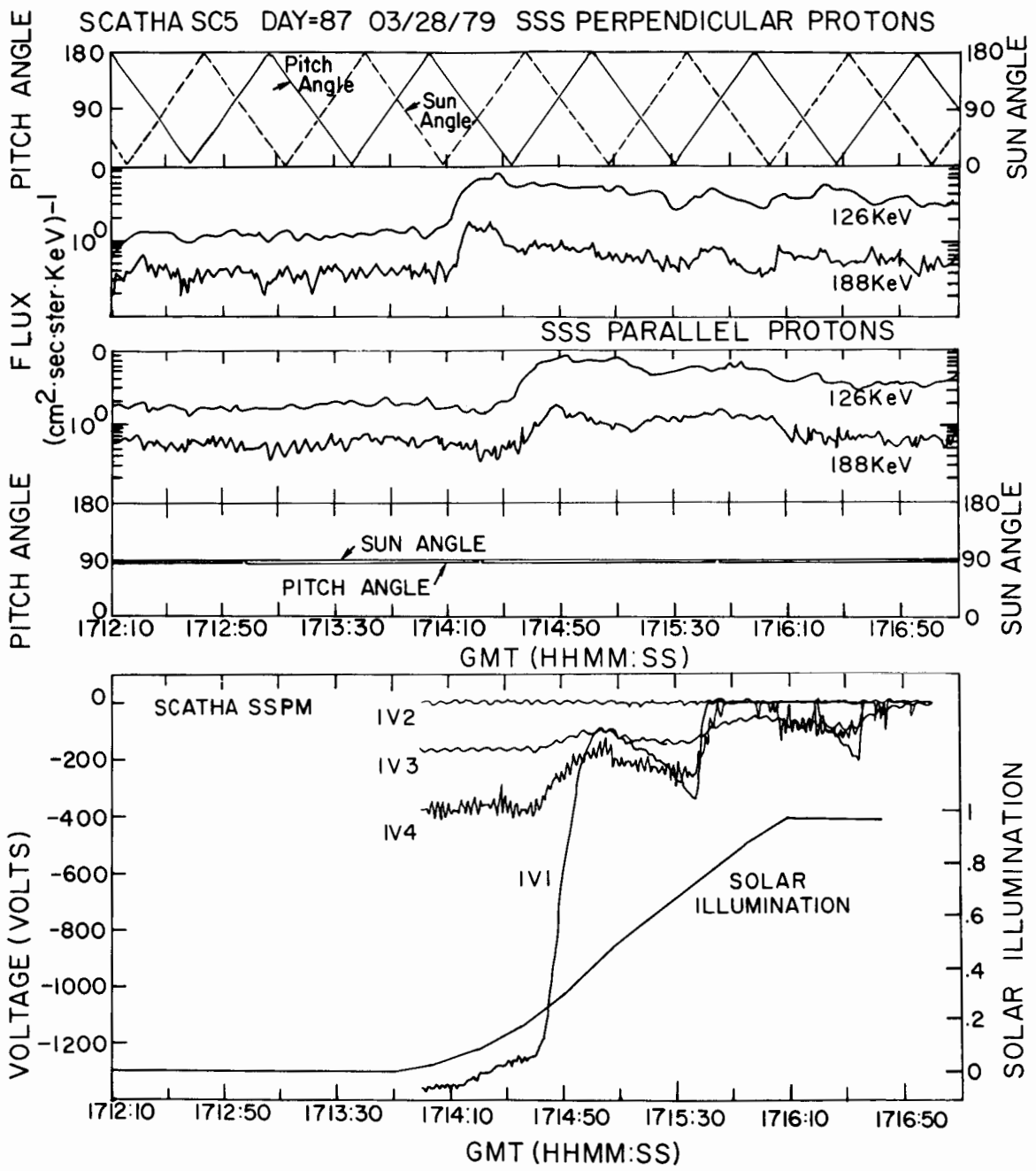

Figure 12. Similar to Figure 10 except for energetic protons and for SSPM-1.

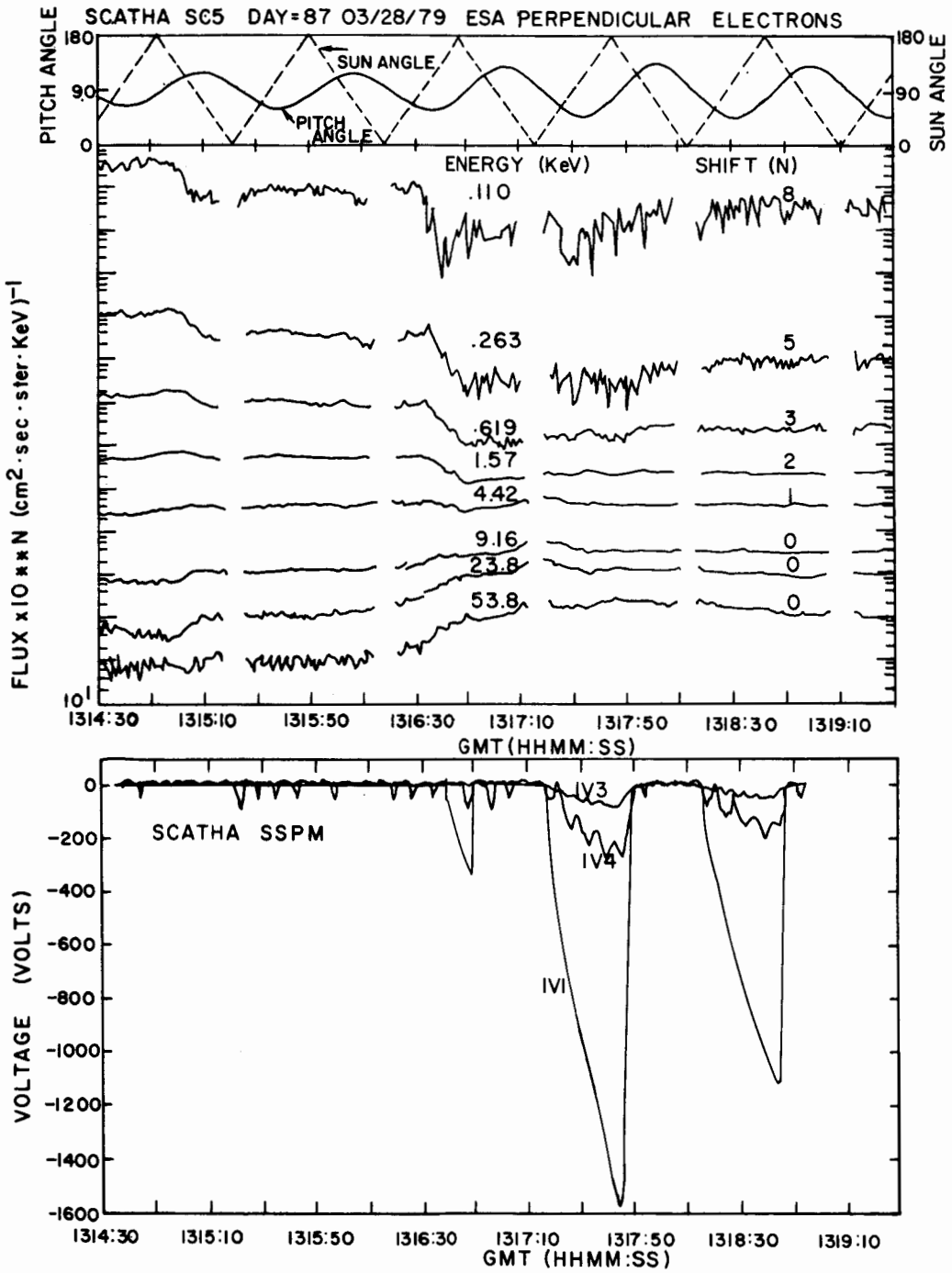

Figure 13. Same as Figure 10 except for energetic ions and for SSPM-1.

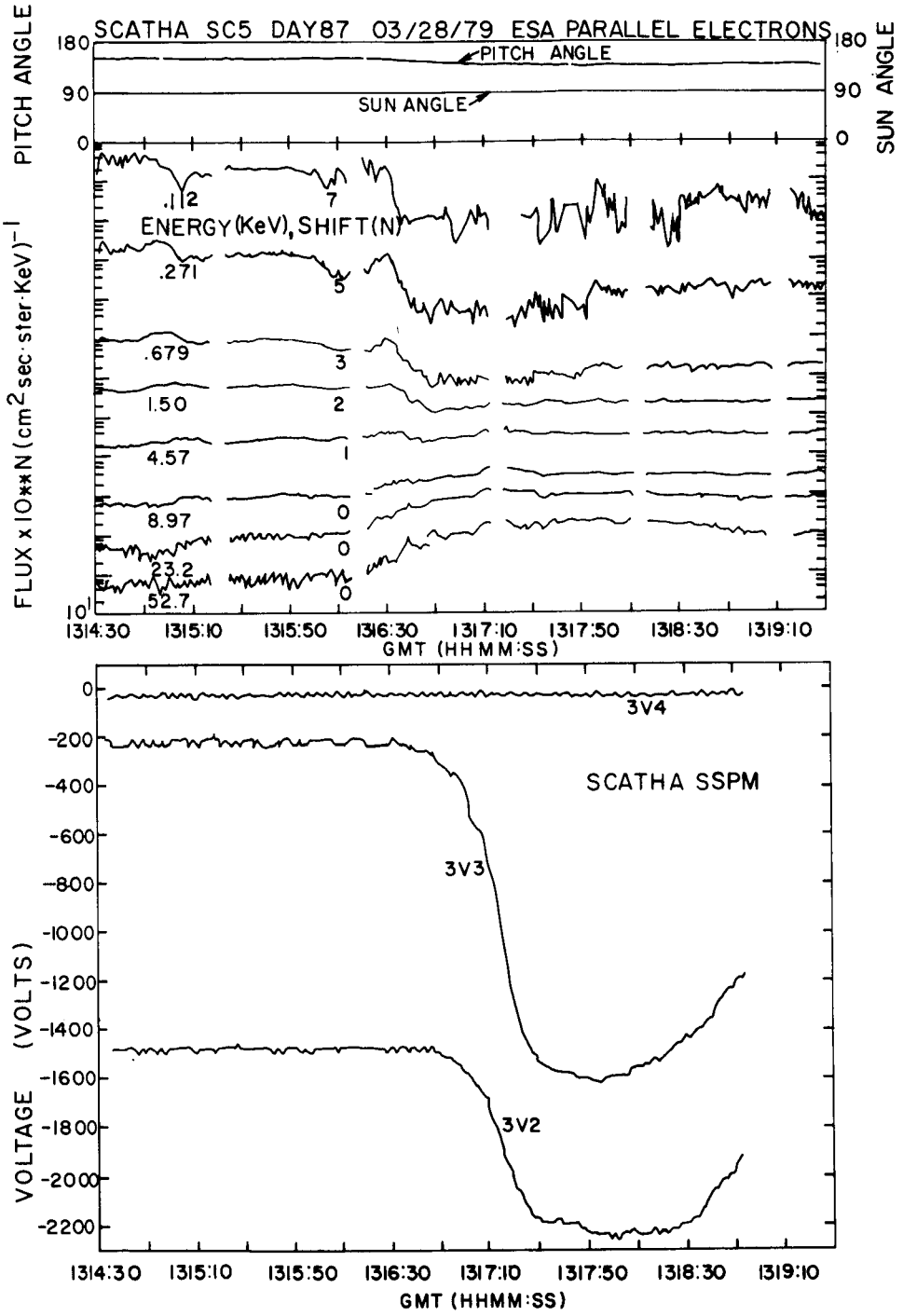

Figure 14. Same as Figure 10 except for parallel electrons and for SSPM-3.

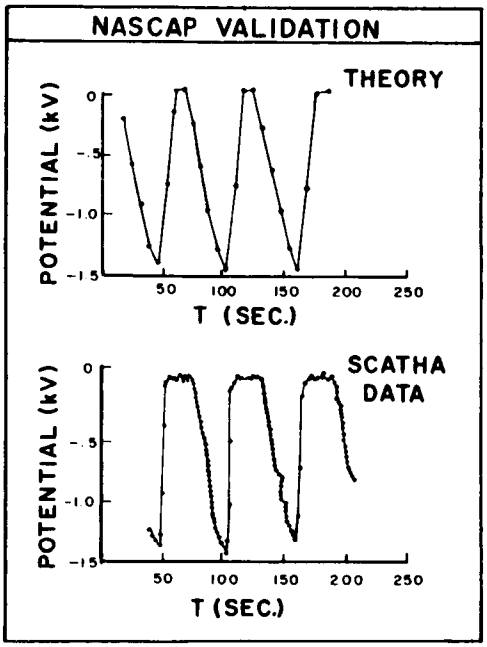

Figure 15. Temporal variation of the kapton sample (SC1-2) potential on the sunlit spinning SCATHA satellite. The upper panel shows the spin modulated potential computed by the NASCAP/AFGL code for the four grid model. The lower panel shows the measured surface potential of kapton in sunlight. The observations were made on day 114, 1979 between 0650:40 and 0653:00 UT.